



ОБЪЕДИНЕННЫЙ
ИНСТИТУТ
ЯДЕРНЫХ
ИССЛЕДОВАНИЙ

Дубна

98-89

E4-98-89

A.B.Arbusov, O.Krehl¹, E.A.Kuraev, E.Magar,
B.G.Shaikhatdenov

RADIATIVE CORRECTIONS
TO THE BACKGROUND OF $\mu \rightarrow e \gamma$ DECAY

Submitted to «Physics Letters B»

¹Institut für Kernphysik, Forschungszentrum, Jülich GmbH,
52425 Jülich, Germany

1998

1 Introduction

Since the discovery of muon in 1936 its relation to electron is a puzzle. Really, the only difference between these two elementary particles is in their masses. The lepton number conservation law has no deep sources in space-time properties or gauge theories. Moreover many extensions of the Standard Model predict processes with violation of this law ($\mu \rightarrow e\gamma$, $e\gamma\gamma$, $e\bar{e}e$ etc.). Intensive search of these extensions was performed in 1977 [1]. The modern state of the subject is elucidated in papers [2, 3] and references therein. Indeed, if there is a unification of quarks and leptons, then the existence of $b \rightarrow s\gamma$ decay leads to that of $\mu \rightarrow e\gamma$. Different models give a wide range of predictions for the branching ratio of this neutrinoless muon decay. The present experimental upper limit [2] on the branching ratio is

$$B = \frac{\Gamma(\mu \rightarrow e\gamma)}{\Gamma_{\mu}^{\text{tot}}} < 4.9 \cdot 10^{-11}. \quad (1)$$

This value imposed already strong restrictions on parameters of supersymmetric [4, 5] and other models [6]. In the model independent approach [7] one gets boundaries on parameters of possible structures in the matrix element of muon decay. Several new experiments are planned to improve the precision. They will either find the decay or put much more stronger restrictions and even discriminate some models. The forthcoming experiment at PSI (if doesn't find the decay) will put the limit on the $\mu \rightarrow e\gamma$ decay branching ratio of about $5 \cdot 10^{-14}$. Another experiment is proposed at BNL, where they are going to reach the level of 10^{-16} . These experiments are very important, since they have rather wide possibilities for the search of new physics comparable with those of high energy colliders. In this paper we consider the important background process

$$\mu(p) \rightarrow e(p_2) + \gamma(k_1) + (\nu_{\mu} + \bar{\nu}_e)(q) \quad (2)$$

in the kinematical situation, imitating the neutrinoless decay. Namely, we suppose

$$n = \frac{2p_2q}{M^2} \sim l = \frac{2k_1q}{M^2} \sim \sqrt{Q^2} = \sqrt{q^2/M^2} \ll 1,$$

where q is the 4-momentum carried by neutrinos, and M is the muon mass. The width in the lowest order of perturbation theory was calculated many years ago [8]. The expression for the width reads:

$$\begin{aligned} d\Gamma_{\text{Born}}^{\mu \rightarrow e\nu\bar{\nu}\gamma} &= \frac{2\alpha G_F^2}{6(2\pi)^6 M} \frac{d^3p_2 d^3k_1}{\varepsilon_2 \omega_1} \left[- \left(\frac{M^4}{2} - q^2 \left(q^2 - \frac{M^2}{2} \right) \right) \left(\frac{p}{pk_1} - \frac{p_2}{p_2k_1} \right)^2 \right. \\ &\quad \left. + 4q^2 + \frac{(k_1q)^2}{(p_2k_1)(pk_1)} (2q^2 + M^2) \right], \quad q = p - p_2 - k_1, \quad \omega_1 = k_1^0. \quad (3) \end{aligned}$$

Validity of this formula may be confirmed in the limiting case of soft photon. Multiplier 2 was lost in right hand side (rhs) of expression for the width in [8]. The

polarized muon radiative decay was considered in [9], and as a background to the neutrinoless decay it was extensively discussed in Ref. [3].

2 Radiative corrections

In the *imitating kinematics* (IK) we introduce the relative energy deviations of hard electron and photon from $M/2$ and the acollinearity angle θ :

$$\sigma_1 = 1 - \frac{2\omega_1}{M}, \quad \sigma_2 = 1 - \frac{2\varepsilon_2}{M}, \quad \theta = \widehat{\mathbf{p}_2, -\mathbf{k}_1}. \quad (4)$$

Here we suggest

$$\sigma_1 \sim \sigma_2 \sim \theta \ll 1. \quad (5)$$

Rearranging the phase volume

$$d\Phi = \frac{d^3 p_2 d^3 k_1}{\omega_1 \varepsilon_2} = 8\pi^2 \left(\frac{M}{2}\right)^4 (1 - \sigma_1)(1 - \sigma_2) d\sigma_1 d\sigma_2 d\theta d\varphi,$$

and expanding expression for width in the Born approximation [9], we obtain:

$$\begin{aligned} \frac{d\Gamma_{\text{Born}}}{d\sigma_1 d\sigma_2 d\theta d\varphi} &= \frac{d\Gamma_0}{d\sigma_1 d\sigma_2 d\theta d\varphi} (1 + \delta_1), \\ \frac{d\Gamma_0}{d\sigma_1 d\sigma_2 d\theta d\varphi} &= \frac{\alpha G_F^2 M^5}{3 \cdot 2^7 \pi^4} R, \quad R = \sigma_2^2 (1 + \xi) + \left(4\sigma_1 \sigma_2 - \frac{\theta^2}{2}\right) (1 - \xi) - \sigma_2 \theta \eta, \\ \xi &= s \cos(\widehat{\mathbf{s}, \mathbf{p}_2}), \quad \eta = s \sin(\widehat{\mathbf{s}, \mathbf{p}_2}) \cos \varphi, \quad \mathbf{k}_1 \mathbf{s} = \omega_1 (-\xi \cos \theta - \eta \sin \theta), \\ \delta_1 &= \frac{1}{R} \left[(-5 + 3\xi) \sigma_1^2 \sigma_2 - 4(1 - \xi) \sigma_2^2 \sigma_1 + 2(1 - \xi) \sigma_1 \theta^2 + \frac{1}{2} (3 - \xi) \sigma_2 \theta^2 \right. \\ &\quad \left. + 4\eta \sigma_1 \sigma_2 \theta - \frac{5}{4} \eta \theta^3 \right]. \end{aligned} \quad (6)$$

Here s denotes spin of the muon, and φ is the azimuthal angle between planes formed by $(\mathbf{s}, \mathbf{p}_2)$ and $(\mathbf{s}, \mathbf{k}_1)$ in a rest frame of muon. Note that averaging the above expression over φ angle, one immediately gets result presented in [3]. We shall name higher than second order contributions in rhs of (3) (and δ_1 in rhs of (6)) as *relativistic* corrections. In this paper we will consider the radiative corrections to this width bearing in mind virtual corrections described by the Feynman diagrams drawn in Fig. 1 together with those arising from emission of additional soft and hard photons.

Taking into account emission of additional hard photon requires to distinguish the cases with or without external magnetic field. In the case without magnetic field the additional hard photon, moving along the final electron trajectory within a small angle, which is equal to the detector angular resolution, is registered together with the electron. In the opposite case (with magnetic field) those events will be

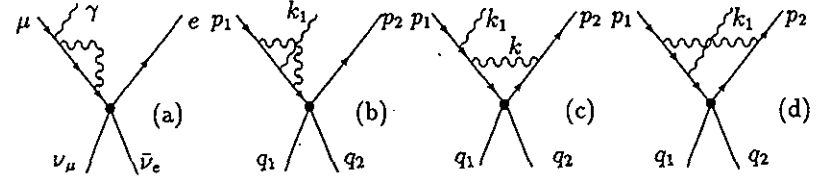


Figure 1: The subset of Feynman diagrams for radiative muon decay.

rejected from statistics, because the energy of the electron will be small. The standard calculation of one-loop virtual corrections can be considerably simplified by using the IK features. Some details of our calculations (traces, vertices and the Tables of relevant integrals) are given in Appendices.

Ultraviolet divergences of loop integrals are eliminated in a standard way using the renormalization constants of the wave functions of electron and muon:

$$\begin{aligned} Z_{1e} &= 1 - \frac{\alpha}{2\pi} \left[\frac{1}{2} \ln \frac{\Lambda^2}{m^2} + \ln \frac{\lambda^2}{m^2} + \frac{9}{4} \right], \\ Z_{1\mu} &= 1 - \frac{\alpha}{2\pi} \left[\frac{1}{2} \ln \frac{\Lambda^2}{M^2} + \ln \frac{\lambda^2}{M^2} + \frac{9}{4} \right], \end{aligned} \quad (7)$$

where m, λ, Λ are the electron mass, infrared and ultraviolet cut-off momentum parameters, respectively ($\lambda \ll m, \Lambda \gg M$). The final result for one-loop virtual corrections reads:

$$\begin{aligned} \frac{d\Gamma^{\text{virt}}}{d\sigma_1 d\sigma_2 d\theta d\varphi} &= \frac{d\Gamma_0}{d\sigma_1 d\sigma_2 d\theta d\varphi} \delta_V, \\ \delta_V &= \frac{\alpha}{\pi R} \left\{ R \left(\frac{3}{2} L - (L-1) \ln \frac{Mm}{\lambda^2} + \frac{\pi^2}{6} \right) + \frac{\sigma_1^2}{4} (1 - \xi) \right. \\ &\quad \left. + \sigma_2^2 \left(-3 - 2L + \frac{\pi^2}{6} \right) (1 + \xi) + \sigma_1 \sigma_2 \left[-\frac{23}{4} + \xi \left(\frac{9}{4} + 4L + \frac{2\pi^2}{3} \right) \right] \right. \\ &\quad \left. + \theta^2 \left[\frac{13}{16} - \xi \left(\frac{3}{16} + \frac{1}{2} L + \frac{\pi^2}{12} \right) \right] + \sigma_2 \theta \eta \left(\frac{7}{4} + 2L \right) - \frac{\pi^2}{12} \sigma_1 \theta \eta \right\}, \\ L &= \ln \frac{M}{m}. \end{aligned} \quad (8)$$

Taking into account the emission of additional soft photon requires some care. The reason is that the energy-momentum carried by soft photons as well as by neutrinos cannot in principle be distinguished in the experiment. We introduce some small energy fraction parameter $\Delta_1 = 2\omega_{\text{soft}}/M \ll \sigma_1, \sigma_2, \theta$ which should not affect on observable quantities and actually cancels out in the final result. Emission of an

additional soft photon having energy lesser than $M\Delta_1/2$ can be taken into account in a usual way [10]. The corresponding expression looks as follows:

$$\frac{d\Gamma^{\text{soft}}}{d^3p_2 d^3k_1} = \frac{d\Gamma_0}{d^3p_2 d^3k_1} \delta_S, \quad \delta_S = \frac{\alpha}{\pi} \left[2(L-1) \ln \frac{2\Delta_1 \epsilon}{\lambda} - L^2 + L + 1 - \frac{\pi^2}{6} \right]. \quad (9)$$

Let us suppose, that a photon with momentum k_2 , having energy more than $\Delta_1 \epsilon$, is emitted in such a way that we have still allowed values of the final electron and hard photon momenta. In this case the additional photon cannot be called soft, because it changes the kinematics of the process. We have to consider the corresponding contribution applying complete set of kinematical restrictions. The main condition is that the missing momentum squared must be positive:

$$\tilde{q}^2 = (p - p_2 - k_1)^2 > 0, \quad \tilde{q} = q + k_2. \quad (10)$$

Having in mind that the matrix element squared is proportional to the second power of small neutrino momenta, we can write down the contribution under consideration in the factorized form

$$\begin{aligned} \frac{d\Gamma^\gamma}{d^3p_2 d^3k_1} &= \frac{d\Gamma_0}{d^3p_2 d^3k_1} \frac{1}{R} \left(-\frac{\alpha}{4\pi^2} \right) \int \frac{d^3k_2}{\omega_2} \left(\frac{p}{pk_2} - \frac{p_2}{p_2k_2} \right)^2 \tilde{R} \Theta(\tilde{q}^2), \\ \tilde{R} &= 2\tilde{Q}^2 + 2\tilde{l}\tilde{n} + \tilde{l}^2 + \xi(-2\tilde{Q}^2 - 2\tilde{l}\tilde{n} + \tilde{l}^2), \\ \tilde{Q}^2 &= \sigma_1\sigma_2 - \frac{1}{4}\theta^2 - x\sigma_1, \quad \tilde{l} = \sigma_2 - x, \quad \tilde{n} = \sigma_1, \\ \tilde{Q}^2 &= \frac{2}{M}\tilde{q}^2, \quad \tilde{l} = \frac{2\tilde{q}p_2}{M}, \quad \tilde{n} = \frac{2\tilde{q}k_1}{M}, \quad x = \frac{2\omega_2}{M}, \quad \omega_2 = k_2^0. \end{aligned} \quad (11)$$

The difference in respect to the case of pure soft photon emission is that we have the *shifted* quantity \tilde{R} instead of the Born one (R) under the integral sign. The above expression guarantees that the energies and angles of the observed electron and photons are the same as defined in (4). Transforming the above formula we get

$$\begin{aligned} \delta_\gamma &= \frac{\alpha}{2\pi} \int_{\Delta_1}^{x_{\text{max}}} \frac{dx}{x} \tilde{R}(x, c_2 = 1) \left[-2 + 4 \ln \left(\frac{M\theta_0}{2m} \right) \right] \Theta \left(\sigma_1\sigma_2 - \frac{\theta^2}{4} - x\sigma_1 \right) \\ &+ \int_0^{2\pi} \frac{d\varphi_2}{2\pi} \int_{-1}^{1-\theta_0^2/2} dc_2 \int_{\Delta_1}^{x_{\text{max}}} \frac{dx}{x} \tilde{R}(x, c_2, \varphi_2) \left(-1 + \frac{2}{1-c_2} \right) \Theta \left(\sigma_1\sigma_2 - \frac{\theta^2}{4} \right. \\ &\left. - \frac{x}{2} (\sigma_1 + \sigma_2 + c_2(\sigma_1 - \sigma_2) - \theta\sqrt{1-c_2^2} \cos \varphi_2) \right), \\ c_2 &= \cos(\hat{k}_2, \hat{p}_2), \quad x_{\text{max}} = \frac{1}{2} \left(\sigma_1 + \sigma_2 + \sqrt{(\sigma_1 - \sigma_2)^2 + \theta^2} \right). \end{aligned} \quad (12)$$

In this expression we introduced an auxiliary parameter θ_0 in order to separate the contribution, when the additional photon is emitted collinear to the electron

momentum; $\theta_0 \ll 1$. So, the first term of Eq. (12) can be integrated analytically in order to keep track of the leading logarithmic part. We checked that the final expression does not depend on θ_0 .

Then we arrive to the total answer, that has the form

$$\frac{d\Gamma}{d\Gamma_0} = 1 + \delta_1 + \delta_V + \delta_S + \delta_\gamma. \quad (13)$$

The dependence on the soft photon parameter Δ_1 cancels out in the sum $\delta_S + \delta_\gamma$, whereas the fictitious photon mass λ disappears in the sum $\delta_S + \delta_V$.

If the experimental set-up does not distinguish in the detector an electron with a collinear photon, we have to modify our results in the following way. Let θ_0 define the aperture of the narrow cone, within which the two particles would be detected as a unique one. Then we should take the *non-shifted* value for R in the first integral of Eq. (12). We have to add also the rest contribution of hard photon emission within the same cone. It can be obtained using the quasireal electron method [11]:

$$\begin{aligned} \frac{d\Gamma^{\text{hard}}}{d\sigma_1 d\sigma_2 \theta d\theta} &= \frac{d\Gamma_0}{d\sigma_1 d\sigma_2 \theta d\theta} \frac{\alpha}{\pi} \int_{x_{\text{max}}}^1 dx \frac{1 + (1-x)^2}{x} \ln \left(\frac{M\theta_0}{2m} \right), \\ x'_{\text{max}} &= \sigma_1 - \frac{\theta^2}{4\sigma_2}. \end{aligned} \quad (14)$$

The lower limit comes here from the Θ -function in the first integral of Eq. (12).

In the presence of a magnetic field, when the electron trajectory is curve, the above expression will give a part of the background to the process $\mu \rightarrow e\gamma\gamma$, considered in paper [12]. Really, the final electron will have the energy $M(1-x)/2$, whereas the quantities $\sigma_1, \sigma_2, \theta$, which characterize the missing energy and momentum, are the same as in the case of single photon emission.

3 Conclusions

In Table 1 we give numerical values for $\delta_1, \delta_{SV\gamma} = \delta_S + \delta_V + \delta_\gamma$ versus $\sigma_1, \sigma_2, \theta$ and ξ . For typical expected values of $\sigma_1 \sim \sigma_2 \sim \theta \sim 10^{-2}$ one can see, that the relativistic and QED corrections should be taken into account on the same footing.

A measurement of the radiative muon decay in the kinematics imitating that of neutrinoless decay is required to get an independent normalization. For this aim our results are very important.

We would like to mention here result obtained in [13] on the background to the three lepton neutrinoless decay $\mu^+ \rightarrow e^+ e^+ e^-$. For an experimental set-up when the electron and positron energies ϵ^\pm are measured, it reads

$$\frac{d\Gamma}{\Gamma_0 d\Delta} = \frac{\alpha^2}{\pi^2} \frac{13}{36} (2-w)^2 \ln \frac{M^2}{m^2}, \quad w = \frac{2}{M} (\epsilon_1^+ + \epsilon_2^+ + \epsilon^-), \quad w \rightarrow 2. \quad (15)$$

\mathcal{N}	$10^2\sigma_1$	$10^2\sigma_2$	$10^2\theta$	$10^2\delta_1$			$10^2\delta_{SV\gamma}$		
				$\xi = 0$	$\xi = 0.5$	$\xi = -0.5$	$\xi = 0$	$\xi = 0.5$	$\xi = -0.5$
1	1.0	1.0	1.0	-1.2	-1.0	-1.3	-10.5	-10.7	-10.3
2	3.0	3.0	3.0	-3.7	-3.0	-4.0	-8.3	-8.5	-8.1
3	5.0	5.0	5.0	-6.1	-5.0	-6.7	-7.2	-7.5	-7.1
4	6.0	6.0	3.0	-10.0	-8.6	-10.8	-6.6	-6.9	-6.5
5	3.0	3.0	5.9	4.4	3.8	4.9	-13.1	-13.2	-13.0
6	4.0	4.0	3.0	-6.0	-5.0	-6.5	-7.5	-7.8	-7.4

Table 1: Numerical estimations for δ_1 and $\delta_{SV\gamma}$ versus $\sigma_1, \sigma_2, \theta$

We have to discuss some features of the results presented. At first we note, that the large logarithm L does not factorize before the Born-like structure (R), as one may expect. We claim that the factorization theorem, which was proved for high energy processes, should not work here. Another problem is that if one integrated out over the whole phase volume of the second photon, he would still have in the answer the logarithm of the mass ratio. Formally, this violates the Kinoshita-Lee-Nauenberg theorem [14]; the formula is infinite in the limit $m \rightarrow 0$. But again, the conditions of the theorem allow us to say, that the process of radiative muon decay is a legal exception. One can see the same situation in radiative muon decay at the Born level [10, 15].

Acknowledgments

One of us (E.A.K.) is grateful for hospitality to Institut für Kernphysik, Jülich, where part of this paper was done and to INTAS 93-239 ext. for financial support.

Appendix A. Tables of integrals

Here we put the tables of relevant integrals appearing in the loop momentum integration. The denominators of amplitudes, which correspond to Feynman diagrams drawn in Fig.1, have the following form:

$$\begin{aligned}
(1) &= (P - k)^2 - M^2, & (2) &= (p_2 - k)^2 - m^2, \\
(\hat{1}) &= (p - k_1 - k)^2 - M^2 \approx k^2 - 2kp_2 - M^2, \\
(\hat{2}) &= (p_2 + k_1 - k)^2 - m^2 \approx k^2 - 2kp + M^2, \\
(0) &= k^2 - \lambda^2.
\end{aligned} \tag{A.1}$$

We use a symbol \approx to underline the peculiarity of imitating kinematics. Namely, working out traces we use

$$p_2^2 = k_1^2 = 0, \quad 2p_2k_1 = M^2 = 1, \quad q = 0. \tag{A.2}$$

The scalar integrals considered have a form

$$\int \frac{dk}{(i)(j)}, \quad \int \frac{dk}{(i)(j)(k)}, \quad \int \frac{dk}{(i)(j)(k)(l)}, \quad dk = \frac{d^4k}{i\pi^2}. \tag{A.3}$$

Vector and tensor integrals are parametrized as follows:

$$\begin{aligned}
\int \frac{k^\mu dk}{N} &= ck_1^\mu + dp_2^\mu, \\
\int \frac{k^\mu k^\nu dk}{N} &= gg^{\mu\nu} + \alpha k_1^\mu k_1^\nu + \beta p_2^\mu p_2^\nu + \gamma (k_1, p_2)^{\mu\nu}, \\
\int \frac{k^\mu k^\nu k^\sigma dk}{N} &= (G^{(1)}(g, k_1) + G^{(2)}(g, p_2) + \kappa (k_1)^3 + \tau (p_2)^3 + \\
&\quad \psi(p_2, k_1, k_1) + \rho(p_2, p_2, k_1))^{\mu\nu\sigma},
\end{aligned} \tag{A.4}$$

where we denote different symmetrical combinations, for instance:

$$(g, a)^{ijk} = g^{ij}a^k + g^{ik}a^j + g^{jk}a^i, \quad (a, b)^{ij} = a^i b^j + a^j b^i, \dots \tag{A.5}$$

Below we put the values of the coefficients and the scalar integrals. In the tables 2 ÷ 7 we used $Y = \ln \frac{A}{M^2}$, $L = \ln \frac{M}{m}$, $X = \frac{\pi^2}{6}$, $Z = \ln \frac{Mm}{\lambda^2}$. All the integrals we put in dimensionless form by setting $M = 1$.

Appendix B. Gauge invariant subset of Feynman diagrams

Amplitudes, describing Feynman diagrams with loop correction to the real photon emission vertex, and the ones, taking into account self-energy of fermions (typical diagrams are shown in Fig.1a,b), provide a gauge invariance in respect to the real photon polarization vector. It has a universal form and may be taken into account by substitutions in Born amplitude of the form

$$\begin{aligned}
\frac{\hat{p} - \hat{k}_1 + M}{-2pk_1} \hat{e}u(p) &\rightarrow \frac{\alpha}{2\pi} \left[A_1 \left(\hat{e} - \hat{k}_1 \frac{pe}{pk_1} \right) + A_2 \hat{k}_1 \hat{e} \right] u(p), \\
A_1 &= \frac{M}{2(M^2 + t)} \left(1 - \frac{t}{M^2 + t} L_t \right), \quad t = -2pk_1, \quad L_t = \log \frac{-t}{M^2}, \\
A_2 &= \frac{N}{t} + \frac{1}{2(t + M^2)} - \frac{2t^2 + 3tM^2 + 2M^4}{2t(M^2 + t)^2} L_t, \\
N &= \frac{M^2}{t} \left[\text{Li}_2(1) - \text{Li}_2\left(\frac{M^2 + t}{M^2}\right) \right], \quad \text{Li}_2(z) = -\int_0^1 \frac{\ln(1 - zx)}{x} dx,
\end{aligned} \tag{B.1}$$

where e is the polarization vector of the real photon. In the IK we have $A_1 = 1/(4M)$, $A_2 = (\pi^2/6 - 1/4)/M^2$. In a similar fashion for the diagrams, which can

be obtained from depicted in Fig.1a,b by emitting a real photon from another leg, we have

$$\bar{u}(p_2) \frac{\hat{p}_2 + \hat{k}_1 + m}{2p_2 k_1} \rightarrow \frac{\alpha}{2\pi} \bar{u}(p_2) \left[B_1 \left(\hat{\epsilon} - \hat{k}_1 \frac{p_2 e}{p_2 k_1} \right) + B_2 \hat{k}_1 \hat{\epsilon} \right]. \quad (\text{B.2})$$

In the IK, omitting the terms disappearing in the limit of zero electron mass, we have $B_1 = 0$, $B_2 = (1/2 - 2L)/M^2$.

Appendix C. Averaging on neutrino states, traces

To rearrange bispinors in the matrix element we use Fierz identity:

$$\bar{u}_1 O_a u_2 \bar{u}_3 O_b u_4 = -\bar{u}_3 O_b u_2 \bar{u}_1 O_a u_4, \quad O_a = \gamma_a(1 + \gamma_5)/2. \quad (\text{C.1})$$

Summing on the neutrino spin states of the matrix element squared one obtains

$$\Sigma \bar{u}_3 O_a u_2 (\bar{u}_3 O_b u_2)^* = 2((q_1 q_2)^{ab} - q_1 q_2 g^{ab}) = L_{ab}. \quad (\text{C.2})$$

Averaging over the neutrino momentum is performed using the invariant integration:

$$\int \frac{d^3 q_1 d^3 q_2}{q_{10} q_{20}} q_1^a q_2^b \delta^4(q_1 + q_2 - q) = \frac{\pi}{6} (q^2 g^{ab} + 2q^a q^b). \quad (\text{C.3})$$

Application of this formula to the tensor L^{ab} gives the result:

$$\int \frac{d^3 q_1 d^3 q_2}{q_{10} q_{20}} L^{ab} \delta^4(q_1 + q_2 - q) = \frac{4\pi}{3} (q^a q^b - q^2 g^{ab}) = \frac{4\pi}{3} O^{ab}. \quad (\text{C.4})$$

The doubled interference term of Born and one-loop amplitudes looks as follows (we consider IK):

$$\frac{1}{2} \int dk \left[\frac{S_1}{(0)(2)(\bar{1})} + \frac{S_2}{(0)(1)(\bar{2})} + \frac{S_3}{(0)(1)(2)(\bar{1})} + \frac{S_4}{(0)(1)(2)(\bar{2})} \right], \quad (\text{C.5})$$

where the traces are:

$$T_i = \frac{1}{4} \text{Tr}(\hat{T}_i^{ac}) O^{ac}, \quad S_i = \frac{1}{4} \text{Tr}(\hat{S}_{i1}^{ac} - \hat{S}_{i2}^{ac}) O^{ac}. \quad (\text{C.6})$$

The list of T_i^{ac} , S_{i1}^{ac} , S_{i2}^{ac} is given below:

$$\begin{aligned} \hat{T}_1 &= \hat{p}_2 \gamma_a (\gamma_b - 2\hat{k}_1 p_b / M^2) (\hat{p} + M) \gamma_b (\hat{p}_2 + M) \gamma_c / M^4, \\ \hat{T}_2 &= \hat{p} + 2\gamma_a \hat{k}_1 \gamma_b (\hat{p} + M) \gamma_b (\hat{p}_2 + M) \gamma_c / M^4, \\ \hat{T}_3 &= \hat{p}_2 \gamma_a \hat{k}_1 \gamma_b \hat{p} \gamma_c \hat{p} \gamma_b / M^4, \end{aligned}$$

(01)	(01)	(02)	(02)	(12)	(12)	(21)	(22)	(11)
$Y+1$	Y	$Y+2L+1$	$Y+1$	Y	Y	Y	$Y+2L-1$	$Y-1$

Table 2: Scalar integrals with 2 denominators

(012)	(011)	(012)	(112)	(012)
$-LZ$	$-X$	$-2L-1$	-1	0

(022)	(122)	(0112)	(0122)
$2L^2 - X$	$1 - 2L$	$2L - X$	$-2L - 2L^2 + X$

Table 3: Scalar integrals with 3 and 4 denominators

	(01)	(01)	(02)	(02)	(12)
d	$\frac{1}{2}Y - \frac{1}{4}$	$\frac{1}{2}Y - \frac{1}{2}$	$\frac{1}{2}Y + L - \frac{1}{4}$	$\frac{1}{2}Y + \frac{1}{4}$	$Y - \frac{1}{2}$
c	$\frac{1}{2}Y - \frac{1}{4}$	0	0	$\frac{1}{2}Y + \frac{1}{4}$	$\frac{1}{2}Y - \frac{1}{2}$

	(12)	(21)	(22)	(11)
d	$Y - \frac{1}{2}$	$Y - \frac{1}{2}$	$Y + 2L - \frac{3}{2}$	$Y - \frac{3}{2}$
c	$Y - \frac{1}{2}$	0	$\frac{1}{2}Y + L - \frac{3}{4}$	$\frac{1}{2}Y - \frac{3}{4}$

Table 4: Vector integrals with 2 denominators

	(012)	(011)	(012)	(112)	(012)
d	$-2L$	$1 - X$	$-L - \frac{1}{4}$	-1	$-\frac{1}{2}$
c	-1	$X - 2$	0	$-\frac{1}{4}$	$-\frac{1}{2}$

	(022)	(122)	(0112)	(0122)
d	$2L^2 - 2L - X$	$1 - 2L$	$2L - X + 1$	$X - 2L^2$
c	$2L - 2$	$-L + \frac{1}{4}$	$X - 1$	$1 - 2L$

Table 5: Vector integrals with 3 and 4 denominators

	(012)	(011)	(012)	(112)	(012)
g	$\frac{1}{4}Y + \frac{1}{8}$	$\frac{1}{4}Y - \frac{1}{2}X + \frac{5}{8}$	$\frac{1}{4}Y$	$\frac{1}{4}Y - \frac{1}{4}$	$\frac{1}{4}Y + \frac{1}{8}$
β	$-L$	$-X + \frac{5}{4}$	$-\frac{2}{3}L - \frac{1}{9}$	-1	$-\frac{1}{2}$
α	$-\frac{1}{4}$	$-X + \frac{3}{2}$	0	$-\frac{1}{9}$	$-\frac{1}{2}$
γ	$-\frac{1}{2}$	$2X - \frac{7}{2}$	0	$-\frac{1}{4}$	$-\frac{1}{2}$

	(022)	(122)	(0112)	(0122)
g	$\frac{1}{4}Y + \frac{3}{8}$	$\frac{1}{4}Y$	$-\frac{1}{2}X + \frac{1}{2}$	$-\frac{1}{4}$
β	$2L^2 - 3L - X + \frac{1}{2}$	$-2L + 1$	$L - X + \frac{5}{4}$	$-2L^2 + 2L + X - \frac{1}{2}$
α	$L - 1$	$-\frac{2}{3}L + \frac{1}{9}$	$-X + \frac{7}{4}$	$-L + \frac{3}{4}$
γ	$2L - \frac{5}{2}$	$-L + \frac{1}{4}$	$2X - 3$	$-2L + 2$

Table 6: 2-rank tensor integrals with 3 and 4 denominators

	$G^{(1)}$	$G^{(2)}$	τ
(0112)	$\frac{1}{2}X - \frac{7}{8}$	$-\frac{1}{2}X + \frac{5}{8}$	$\frac{2}{3}L - X + \frac{49}{36}$
(0122)	$-\frac{1}{8}$	$-\frac{1}{4}$	$-2L^2 + 3L + X - 1$
	κ	ρ	ψ
(0112)	$X - \frac{29}{18}$	$3X - \frac{19}{4}$	$-3X + 5$
(0122)	$-\frac{2}{3}L + \frac{11}{18}$	$-2L + \frac{5}{2}$	$-L + 1$

Table 7: 3-rank tensor integrals with 4 denominators

$$\begin{aligned}
S_{31} &= (\hat{p} + 1)\gamma_c \hat{p} \gamma_b \hat{p}_2 \gamma_\mu (\hat{p}_2 - \hat{k}) \gamma_a (\hat{p}_2 - \hat{k} + 1) \gamma_b (\hat{p} - \hat{k} + 1) \gamma_\mu, \\
S_{12} &= (\hat{p}_2 + 1) \gamma_b (\hat{p} + 1) \gamma_c \hat{p} \gamma_b \hat{p}_2 \gamma_\mu (\hat{p}_2 - \hat{k}) \gamma_a (\hat{p}_2 - \hat{k} + 1) \gamma_\mu, \\
S_{21} &= (\hat{p} + 1) \gamma_c \hat{p} \gamma_b \hat{p}_2 \gamma_b \hat{p} \gamma_\mu (\hat{p} - \hat{k}) \gamma_a (\hat{p} - \hat{k} + 1) \gamma_\mu, \\
S_{41} &= (\hat{p} + 1) \gamma_c \hat{p} \gamma_b \hat{p}_2 \gamma_\mu (\hat{p}_2 - \hat{k}) \gamma_b (\hat{p} - \hat{k}) \gamma_a (\hat{p} - \hat{k} + 1) \gamma_\mu, \\
S_{32} &= (\hat{p} + 1) \gamma_b (\hat{p}_2 + 1) \gamma_c \hat{p}_2 \gamma_\mu (\hat{p}_2 - \hat{k}) \gamma_a (\hat{p}_2 - \hat{k} + 1) \gamma_b (\hat{p} - \hat{k} + 1) \gamma_\mu, \\
S_{42} &= (\hat{p} + 1) \gamma_b (\hat{p}_2 + 1) \gamma_c \hat{p}_2 \gamma_\mu (\hat{p}_2 - \hat{k}) \gamma_b (\hat{p} - \hat{k}) \gamma_a (\hat{p} - \hat{k} + 1) \gamma_\mu, \\
S_{11} &= (\hat{p}_2 + 1) \gamma_b (\hat{p} + 1) \gamma_b (\hat{p}_2 + 1) \gamma_c \hat{p}_2 \gamma_\mu (\hat{p}_2 - \hat{k}) \gamma_a (\hat{p}_2 - \hat{k} + 1) \gamma_\mu, \\
S_{22} &= (\hat{p} + 1) \gamma_b (\hat{p}_2 + 1) \gamma_c \hat{p}_2 \gamma_b \hat{p} \gamma_\mu (\hat{p} - \hat{k}) \gamma_a (\hat{p} - \hat{k} + 1) \gamma_\mu.
\end{aligned}$$

$$S_1 = S_{11} - S_{12}, \quad S_2 = S_{21} - S_{22}, \quad S_3 = S_{31} - S_{32}, \quad S_4 = S_{41} - S_{42}. \quad (C.7)$$

References

- [1] B. Lee et al., Phys. Rev. Lett. **38** (1977) 937;
S.T. Petkov, Sov. J. Nucl. Phys. **25** (1977) 340;
T. Cheng and L.-F. Li, Phys. Rev. Lett. **38** (1977) 381;
H. Fritzsch, Phys. Lett. **B 67** (1977) 451.
- [2] R.D. Bolton et al., Crystal Box Coll., Phys. Rev. **D 38** (1988) 2077.
- [3] Y. Kuno, A. Maki, Y. Okada, Phys. Rev. **D 55** (1997) 2517;
Y. Kuno, Y. Okada, Phys. Rev. Lett. **77** (1996) 434.
- [4] R. Barbieri, L. Hall, A. Strumia, Nucl. Phys. **B 445** (1995) 219, and references therein.
- [5] J. Hisano, T. Moroi, K. Tobe et al., Phys. Rev. **D 53** (1996) 2442.
- [6] J.D. Vergados, Phys. Rep. **133** (1986) 1;
R.N. Mohapatra, Phys. Rev. **D 46** (1992) 2990.
- [7] M.V. Chizhov, Mod. Phys. Lett. **A 9** (1994) 2979; hep-ph/9612399, and references therein.
- [8] A. Lenard, Phys. Rev. **90** (1953) 968.
- [9] C. Fronsdal, H. Überall, Phys. Rev. **113** (1959) 654;
S. Eckstein, R. Pratt, Ann. Phys. (NY) **8** (1959) 297.
- [10] A.I. Akhiezer and V.B. Berestetsky, Quantum Electrodynamics, 1981, Moscow.

- [11] V.N. Baier, V.F. Fadin, V.A. Khoze, Nucl.Phys. **B 65** (1973) 381.
- [12] L.A. Vassilevskaia et al., Phys. Lett. **B 267** (1991) 121.
- [13] A. Arbuzov, E. Kuraev, N. Merenkov, N. Makhaldiani, JETP Lett. **57** (1993) 746.
- [14] T. Kinoshita, J. Math. Phys. (N.Y.) **3** (1962) 650;
T.D. Lee and M. Nauenberg, Phys. Rev. **133** (1964) 1549.
- [15] S.M. Berman, A. Sirlin, Ann. Phys. (NY) **20** (1962) 20.

Received by Publishing Department
on April 10, 1998.